

Diffusion pore imaging with generalized temporal gradient profiles.

Frederik Bernd Laun^{1,2}, Tristan Anselm Kuder¹

1) Medical Physics in Radiology, German Cancer Research Center (DKFZ), Im Neuenheimer Feld 280,
69120 Heidelberg, Germany

2) Quantitative Imaging-Based Disease Characterization, German Cancer Research Center (DKFZ), Im
Neuenheimer Feld 280, 69120 Heidelberg, Germany

Abstract

In porous material research, one main interest of nuclear magnetic resonance diffusion (NMR) experiments is the determination of the exact shape of pores. While it has been a longstanding question if this is in principle achievable, it has been shown recently that it is indeed possible to perform NMR-based diffusion pore imaging. In this work we present a generalization of these previous results. We show that the specific temporal gradient profiles that were used so far are not unique as almost arbitrary temporal diffusion gradient profiles may be used.

Nuclear magnetic resonance (NMR) based diffusion experiments find widespread application in medical imaging and porous media research as the measured diffusion-weighted signal allows one to infer information about structures restricting the diffusion process [1,2,3]. For a long time, it has been an open question if NMR diffusion experiments could exactly reveal the shape of the boundary of closed pores [4]. In a recent publication [5], we could show that this is indeed possible, if the temporal antisymmetry of the diffusion weighting magnetic field gradients is broken by using one long and one short diffusion weighting gradient pulse (gradient profile $G_{\text{long-narrow}}(t)$, see Fig. 1). In a porous sample with many closed pores of similar shape filled with an NMR visible medium, this technique can be applied to obtain an image of the pore geometry averaged over the considered volume element. Compared to conventional NMR imaging, largely increased signal-to-noise ratios can be achieved, since the signal can be collected from the whole sample. Shortly after publication of this first approach, Shemesh et al. [6] proposed another reconstruction approach that is based on multiple wave-vector diffusion weightings [7,8], for which Özarlan and Basser previously recognized that the signal could contain phase information about the pore shape [9]. Shemesh et al. [6] used a gradient profile consisting of three short gradient pulses ($G_{121}(t)$, see Fig. 1). Using their image reconstruction approach, this profile, in combination with the classical q-space profile [10,11] consisting of two short gradients ($G_{11}(t)$, see Fig. 1), can be used to infer the pore space function if one knows a priori that the pore space function is point symmetric. We generalized these results and showed that the pore space function can be retrieved using the profile $G_{121}(t)$ without the need to assume point symmetry of the domain, and without the need to acquire additional data with the profile $G_{11}(t)$ [12].

It is a natural question to ask if these proposed gradient profiles have extraordinary properties, which allow for imaging pore shapes, or if the main aspect is the broken temporal antisymmetry. In the latter case, one may ask which further gradient profiles are suitable to retrieve the shape of the pore space function. Answers to these questions may be helpful to assess which acquisition scheme is best

suited for a specific application. In this technical note, we show that in principle almost arbitrary temporal gradient profiles can be used as long as they contain at least one sharp gradient pulse.

Assume that the gradient profile

$$\mathbf{G}(t) = \mathbf{G}_0(t) + \gamma^{-1} \mathbf{q} \sum_{n=1}^N c_n \delta(t - t_n) \quad (1)$$

is used, where γ is the gyromagnetic ratio. $\mathbf{G}_0(t)$ is an arbitrary “small” gradient. A more thorough discussion of the term “small” and the small gradient can be found in [13] in section 4.1. In particular, $\mathbf{G}_0(t)$ should not contain Dirac delta functions and should not induce a considerable diffusion weighting effect on its own. The constants c_n are real and one of them is equal to one, all others must be smaller than one and larger than minus one. The parameter $c_n \mathbf{q}$ specifies the wave-vector that is generated by the gradient pulse applied at time t_n , which is represented by the Dirac delta function $\delta(t - t_n)$. In general, the relation between a gradient pulse $\mathbf{G}_n(t)$ and its associated wave-vector is $\mathbf{q}_n = \gamma \int \mathbf{G}_n(t) dt$. The separation of the Dirac delta pulses must be “long”, which means $|t_n - t_{n-1}| \gg L^2 / D$ for all t_n , where D is the free diffusion coefficient. L is the length of the domain, for instance, the radius of a sphere. The upper bound N is an arbitrary integer greater than or equal to one. As usual, the Dirac delta functions are considered as the limiting case of very strong and short diffusion gradients. It is further assumed that the rephasing condition is fulfilled:

$$\int_0^T \mathbf{G}(t) dt = 0 \quad (2)$$

Here, T is the total duration of the gradient profile. We introduce the pore space function $\chi(\mathbf{x})$, which is one inside and zero outside the domain. $P(\mathbf{x}_2, \mathbf{x}_1, \Delta t)$ denotes the propagator function indicating the probability for a particle to travel from \mathbf{x}_1 to \mathbf{x}_2 in the time Δt . First assume that the

small gradient $\mathbf{G}_0(t)$ is zero. Then at least two short gradient pulses must be applied to fulfill the rephasing condition and the obtained signal is

$$S(\mathbf{q}) = \int d\mathbf{x}_1 \frac{\chi(\mathbf{x}_1)}{V} e^{-i\mathbf{q}_1 \mathbf{x}_1} \prod_{n=2}^N \left(\int d\mathbf{x}_n \right) \prod_{n=2}^N \left(P(\mathbf{x}_n, \mathbf{x}_{n-1}, t_n - t_{n-1}) e^{-i\mathbf{q}_n \mathbf{x}_n} \right), \quad (3)$$

with $\mathbf{q}_n = \mathbf{q}c_n$. If $|t_n - t_{n-1}| \gg L^2 / D$, the correlations of the positions \mathbf{x}_n and \mathbf{x}_{n-1} are lost yielding $P(\mathbf{x}_n, \mathbf{x}_{n-1}, t_n - t_{n-1}) = \chi(\mathbf{x}_n) / V$. Thus, Eq. (3) becomes

$$S(\mathbf{q}) = \frac{1}{V^N} \prod_{n=1}^N \int d\mathbf{x}_n \chi(\mathbf{x}_n) e^{-i\mathbf{q}_n \mathbf{x}_n}, \quad (4)$$

which is equal to

$$S(\mathbf{q}) = \prod_{n=1}^N \tilde{\chi}(\mathbf{q}_n) = \prod_{n=1}^N \tilde{\chi}(\mathbf{q}c_n), \quad (5)$$

where $\tilde{\chi}(\mathbf{q}_n)$ is the Fourier transform of the pore space function $\chi(\mathbf{x}_n)$:

$$\tilde{\chi}(\mathbf{q}_n) = \frac{1}{V} \int d\mathbf{x}_n \chi(\mathbf{x}_n) e^{-i\mathbf{x}_n \mathbf{q}_n} \quad (6)$$

Note that $\tilde{\chi}(-\mathbf{q}_n) = \tilde{\chi}^*(\mathbf{q}_n)$, where the star denotes the complex conjugate, since $\chi(\mathbf{x}_n)$ is real.

If the small gradient is not zero, then, as laid out in [5,13], Eq. (5) must be modified with a phase factor $e^{-i\mathbf{q}_0 \mathbf{x}_{cm}}$

$$S(\mathbf{q}) = e^{-i\mathbf{q}_0 \mathbf{x}_{cm}} \prod_{n=1}^N \tilde{\chi}(\mathbf{q}_n) = e^{-i\mathbf{q}_0 \mathbf{x}_{cm}} \prod_{n=1}^N \tilde{\chi}(c_n \mathbf{q}), \quad (7)$$

where \mathbf{x}_{cm} is the center of mass of the domain, and \mathbf{q}_0 is

$$\mathbf{q}_0 = \gamma \int_0^T \mathbf{G}_0(t) dt. \quad (8)$$

Due to the rephasing condition, identical pores at different locations yield identical signals; all pores seem to be shifted to the same location. Thus, for the image reconstruction, it may be assumed without loss of generality that the pore is placed such that the center of mass is at the coordinate origin, such that $e^{-iq_0x_{cm}} = 1$.

The task is to solve Eq. (5) for $\tilde{\chi}(\mathbf{q})$. If N was equal to one, the solution would be straightforwardly obtained by Fourier transformation as described in [5,13]. If N is larger than one, we assume that m is the index for which $c_m = 1$. Thus, $\mathbf{q}_m = c_m \mathbf{q} = \mathbf{q}$ is the largest of the values \mathbf{q}_n and we rewrite Eq. (5) as

$$\tilde{\chi}(\mathbf{q}) = S(\mathbf{q}) / \prod_{n=1, n \neq m}^N \tilde{\chi}(\mathbf{q}_n). \quad (9)$$

This is an equation that can be solved iteratively if $S(\mathbf{q})$ is known from experiments, and if $\tilde{\chi}(\mathbf{q}_n)$ is known for some initial small \mathbf{q}_n -values. Considering Eq. (6), one finds $\tilde{\chi}(\mathbf{0}) = 1$. $\tilde{\chi}(\mathbf{q}_n)$ can be expanded in a series for small q -values. As laid out in [12], one has freedom in specifying the term linear in \mathbf{q}_n as this term specifies the position of the reconstructed pore. If this linear term is set to zero, the pore is reconstructed such that its center of mass is located on the origin. By these considerations, $\tilde{\chi}(\mathbf{q}_n)$ is fully specified for small q -values, and the iterative solution of Eq. (9) is possible and unique by setting $\tilde{\chi}(\mathbf{q}_n) = 1$ for the initial small values of \mathbf{q}_n .

For demonstration purposes, we chose the four temporal gradient profiles $G_{12}(t)$, $G_{123}(t)$, $G_{235}(t)$ and $G_{1113}(t)$ (see Fig. 1, δ is the duration of the short gradient pulse). Simulations based on the multiple correlation function technique [4,13,14,15,16,17,18] were performed using the hemi-equilateral domain (see Fig. 2). The following computation parameters were chosen: Free diffusion coefficient $D = 1 \mu\text{m}^2/\text{ms}$, length of edge $L = 20 \mu\text{m}$, $T = 100$ s, duration of the short gradient pulses 0.1 ms, 76 eigenvalues. The q -space was sampled radially along 180 isotropically distributed directions, the

maximal q-value \mathbf{q}_{\max} was $4.1 \mu\text{m}^{-1}$, and data points at 400 q-values were acquired in equidistant steps of the q-value for each spoke. The image was reconstructed by inverse radon transformation for a field of view of $31.4 \mu\text{m}$. Eq. (9) was solved iteratively. A basic iteration scheme without outlier rejection etc. was used. The initial two of the 400 values of $\tilde{\chi}(\mathbf{q})$ were set to 1 in order to be able to start the iteration.

Figure 2 shows the reconstructed images, which are all of good quality. The triangular shape is clearly visible and little reconstruction artifacts are observable.

Thus it turns out that the pore space function can be detected with almost arbitrary temporal gradient profiles using the iterative approach presented here, excluding two important cases. First, at least one short gradient pulse must be present, because, otherwise, no $\tilde{\chi}(\mathbf{q}_n)$ -term appears in Eq. (5). Second, the iterative reconstruction of Eq. (9) is not possible if all short gradients generate the same wave vector, or wave vectors of opposite sign. Thus, classical q-space imaging gradients are not suitable for this approach.

The here presented findings are foremost of theoretical interest, but some comments regarding practical implementations are in order. First, it should be noted that the iterative reconstruction of Eq. (9) is crucially depending on the exact cancellation of the signal $S(\mathbf{q})$ and of $\tilde{\chi}(\mathbf{q}_n)$ at the zero crossings of $\tilde{\chi}(\mathbf{q}_n)$. This is not a problem under ideal conditions, since $S(\mathbf{q}) = 0$ if there is a value for n for which $\tilde{\chi}(\mathbf{q}_n) = 0$. Measurements, however, are not ideal in two regards. First, measurement noise is present, and second, the actual $S(\mathbf{q})$ deviates from the theoretical $S(\mathbf{q})$, since the short diffusion gradients are not really infinitesimally, and since the total duration T is not infinite. The hemi-equilateral triangle is a benign domain in this regard, since zero crossings of $\tilde{\chi}(\mathbf{q}_n)$ are sparse, but, for instance, cylindrical and spherical domains are much more prone to “no-cancellation artifacts” as $\tilde{\chi}(\mathbf{q}_n)$ exhibits many zero crossings. This can be circumvented by

straightforward approaches such as, for example, assuming the actual pore shape is known a priori, which allows a direct fit as described in [6]. Otherwise, it may be necessary to implement sophisticated reconstruction algorithms.

What is the ideal number of short gradient pulses in real experiments? In our opinion, there are basically two options. The first option is to use only one short gradient pulse. This is beneficial since the iterative reconstruction using Eq. (9) is not required, and since a Fourier transformation can be used to retrieve the pore image straightforwardly. Using only one short gradient comes at two big costs. First, a long small gradient must be used, which rules out any attempt to use stimulated echoes (e.g. [19,20,21]), and thus reduces the available sequence options. Second, the convergence towards the long-time limit, in which a sharp image can be reconstructed, is slower than with short gradient pulses only. Details on convergence properties are described in [13]. Both these complications can be avoided using only narrow gradient pulses and the iterative reconstruction, which, however, is less stable than the one-pulse Fourier transform [12]. Since the reconstruction becomes even more unstable with increasing number of pulses, the used number of pulses should be as small as possible. Thus, three narrow pulses should be used. Two narrow gradient pulses alone cannot fulfill the rephasing condition since the gradient pulses are required to generate different q -values.

In conclusion, we showed that the shape of arbitrary pores can be retrieved with quite general diffusion gradient profiles. The profiles presented in previous works [5,6,12,13] are thus not special, and one has freedom in shaping the gradient profile to match experimental conditions. Two questions remain open. First, is there a gradient profile without sharp gradient pulse that can be used to retrieve the pore space function? Such an approach would presumably reduce the demands on the gradient system. And second, how much information can be gained in open and permeable systems? Answers to these questions would be highly valuable.

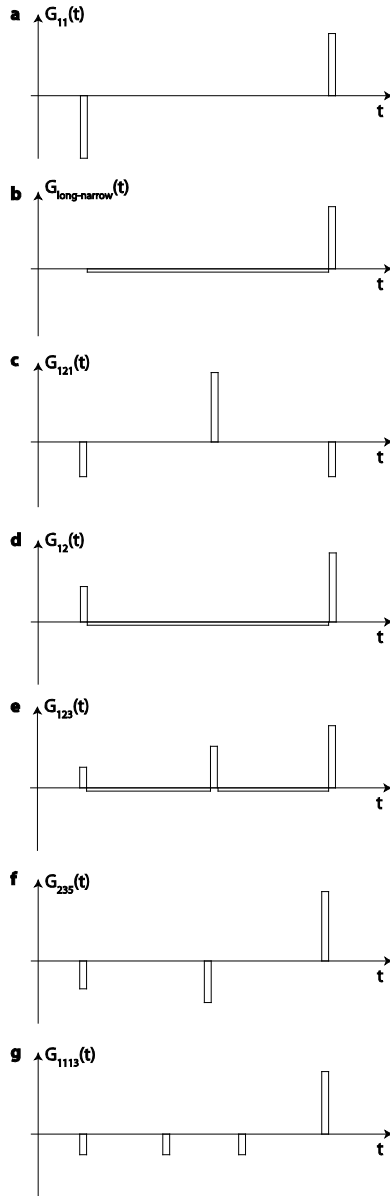


Figure 1. The gradient profiles used in this manuscript. a) Classical q-space gradients $G_{11}(t)$. b) “Long-narrow” gradients $G_{\text{long-narrow}}(t)$ consisting of one long and one narrow gradient pulse. The zeroth moment of both gradient pulses cancel in order to fulfill the rephasing condition. c) Gradient profile $G_{121}(t)$ consisting of three narrow gradient pulses. d) Gradient profile $G_{12}(t)$ consisting of two narrow and one long gradient pulse. e) Gradient profile $G_{123}(t)$. The relative zeroth moment of the narrow gradient pulses is $1/2/3$. f) Gradient profile $G_{235}(t)$ consisting of three narrow gradient pulses with relative zeroth moments of $-2/-3/5$. g) Gradient profile $G_{1113}(t)$ consisting of four narrow gradient pulses with relative zeroth moments of $-1/-1/-1/3$.

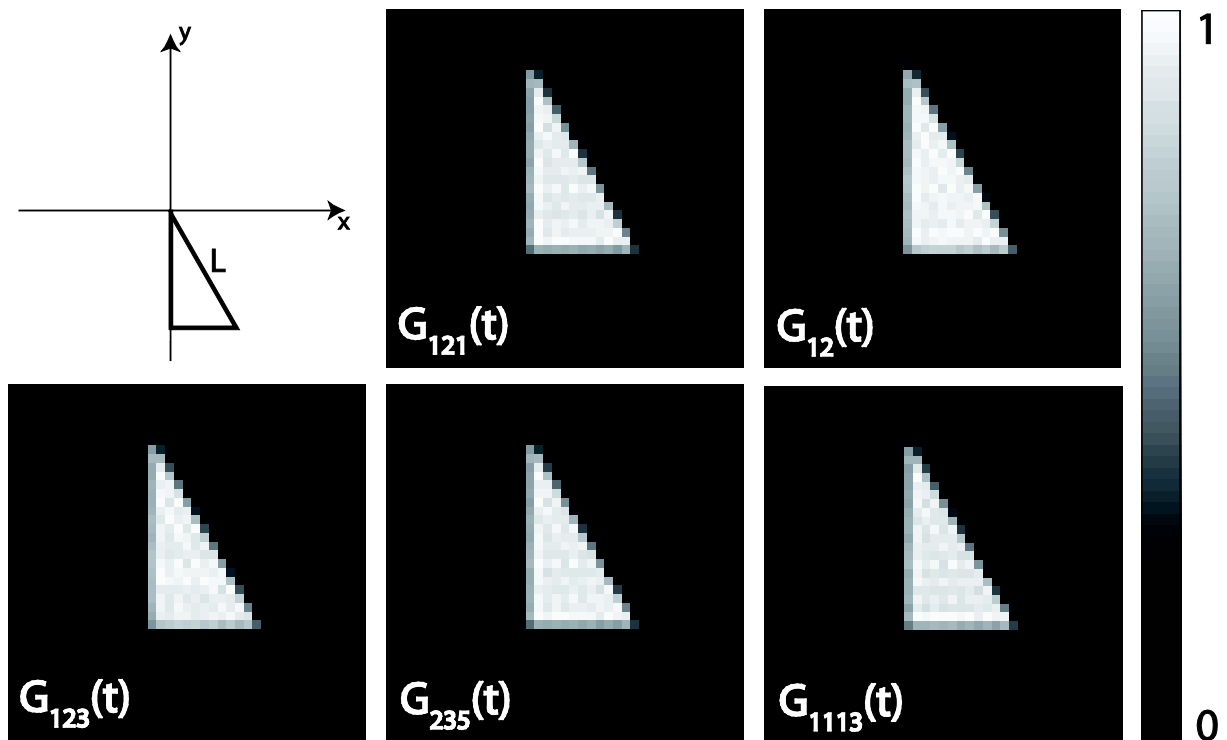


Figure 2. Diffusion pore images obtained for the hemi-equilateral triangle depicted in the upper left sketch with a variety of gradient profiles. The images are of high quality for all gradient profiles. Images were min-max normalized.

1. Callaghan PT (2011) *Translational Dynamics & Magnetic Resonance*: Oxford University Press.
2. Stejskal EO (1965) Use of spin echoes in a pulsed magnetic-field gradient to study anisotropic, restricted diffusion and flow. *J Chem Phys* 43: 3597-3603.
3. Sen PN (2004) Time-dependent diffusion coefficient as a probe of geometry. *Concepts in Magnetic Resonance Part A* 23: 1-21.
4. Grebenkov DS (2007) NMR survey of reflected Brownian motion. *Reviews of Modern Physics* 79: 1077-1137.
5. Laun FB, Kuder TA, Semmler W, Stieltjes B (2011) Determination of the defining boundary in nuclear magnetic resonance diffusion experiments. *Phys Rev Lett* 107: 048102.
6. Shemesh N, Westin CF, Cohen Y (2012) Magnetic resonance imaging by synergistic diffusion-diffraction patterns. *Phys Rev Lett* 108: 058103.
7. Mitra PP (1995) Multiple Wave-Vector Extensions of the Nmr Pulsed-Field-Gradient Spin-Echo Diffusion Measurement. *Physical Review B* 51: 15074-15078.
8. Özarlan E, Bassler PJ (2008) Microscopic anisotropy revealed by NMR double pulsed field gradient experiments with arbitrary timing parameters. *J Chem Phys* 128: 154511.
9. Özarlan E, Bassler PJ (2007) MR diffusion - "diffraction" phenomenon in multi-pulse-field-gradient experiments. *J Magn Reson* 188: 285-294.
10. Callaghan PT, Macgowan D, Packer KJ, Zelaya FO (1990) High-Resolution Q-Space Imaging in Porous Structures. *Journal of Magnetic Resonance* 90: 177-182.
11. Cory DG, Garroway AN (1990) Measurement of translational displacement probabilities by NMR: an indicator of compartmentation. *Magn Reson Med* 14: 435-444.
12. Kuder TA, Laun FB (2012) NMR Based Diffusion Pore Imaging by Double Wave Vector Measurements. [arXiv:1205.1793v1](https://arxiv.org/abs/1205.1793v1).
13. Laun FB, Kuder TA, Stieltjes B, Semmler W (2012) NMR-based diffusion pore imaging. *Phys Rev E* (accepted).
14. Axelrod S, Sen PN (2001) Nuclear magnetic resonance spin echoes for restricted diffusion in an inhomogeneous field: Methods and asymptotic regimes. *J Chem Phys* 115: 6878-6895.
15. Barzykin AV (1999) Theory of spin echo in restricted geometries under a step-wise gradient pulse sequence. *J Magn Reson* 139: 342-353.
16. Grebenkov DS (2008) Analytical solution for restricted diffusion in circular and spherical layers under inhomogeneous magnetic fields. *Journal of Chemical Physics* 128: 134702.
17. Grebenkov DS (2010) Pulsed-gradient spin-echo monitoring of restricted diffusion in multilayered structures. *Journal of Magnetic Resonance* 205: 181-195.
18. Laun FB (2012) Restricted diffusion in NMR in arbitrary inhomogeneous magnetic fields and an application to circular layers. *J Chem Phys*: 044704.
19. Hiepe P, Herrmann KH, Ros C, Reichenbach JR (2011) Diffusion weighted inner volume imaging of lumbar disks based on turbo-STEAM acquisition. *Z Med Phys* 21: 216-227.
20. Cotts RM, Hoch MJR, Sun T, Markert JT (1989) Pulsed Field Gradient Stimulated Echo Methods for Improved NMR Diffusion Measurements in Heterogeneous Systems. *Journal of Magnetic Resonance* 83: 252-266.
21. Yongbi MN, Ding S, Dunn JF (1996) A modified sub-second fast-STEAM sequence incorporating bipolar gradients for in vivo diffusion imaging. *Magn Reson Med* 35: 911-916.